ISSN 0915-633X

NATIONAL INSTITUTE FOR FUSION SCIENCE

Measurement of the Poloidal Magnetic Field Profile with High Time Resolution Zeeman Polarimeter in the JIPP T-IIU Tokamak

H. Kuramoto, N. Hiraki, S. Moriyama, K. Toi, K. Sato,
K. Narihara, A. Ejiri, T. Seki and JIPP T-IIU Group

(Received - Jan. 25, 1996)

NIFS-397 Feb. 1996

RESEARCH REPORT
NIFS Series

NAGOYA, JAPAN

The seventh International Toki Conference on Plasma Physics and Controlled Nuclear Fusion (To be published in Fusion Engineering and Design)

Measurement of the Poloidal Magnetic Field Profile with High Time Resolution Zeeman Polarimeter in the JIPP T-IIU Tokamak

H.Kuramoto[1)], N.Hiraki[1)], S.Moriyama[1)], K.Toi, K.Sato, K.Narihara,

A.Ejiri, T.Seki and JIPP T-IIU Group

National Institute for Fusion Science, Nagoya, 464-01, Japan

1) Kyushu Institute of Technology, Iizuka, 820, Japan

ABSTRACT

A Zeeman polarimeter with high time resolution is developed to measure poloidal magnetic field of a tokamak plasma from the analysis of circular polarization of HeII 4686Å. The polarimeter is successfully applied to fast current ramping experiments in He-doped deuterium plasmas of JIPP T-IIU.

Key Words: Poloidal magnetic field profile measurement, High time resolution Zeeman polarimeter, Circular polarization, Current ramp experiment, JIPP T-IIU

1. Introduction

The experiments for controlling the local plasma current density profile have been carried out in various ways[1-6] in many tokamaks to investigate the effect of the current density profile on plasma confinement. In JIPP T-IIU, the current density profile is controlled with rapid ramp up or ramp down of the plasma current. In order to measure the current density profile in such tokamak experiments, we constructed a Zeeman polarimeter with high time resolution. The polarimeter consists of a photoelastic modulator, a fast scanning Fabry-Perot interferometer and so on[7].

The internal poloidal magnetic field prescribed by the current density profile is generally deduced from a polarization analysis of the spectral line emitted from a plasma[8,9]. When we observe the spectral line in the direction along the magnetic field line, we can find each component of the left-hand and right-hand circular polarizations in the spectral line. The maximum difference between modulation ratios on the polarizations opposite each other is directly proportional to the magnetic field component in the observation direction. Therefore, if we set many observation directions in the tokamak poloidal plane, we can easily determine the poloidal magnetic field distribution, that is, the toroidal current density profile from measuring the polarization modulation. So, according to such principle, we tried applying the developed polarimeter to He-doped plasmas in JIPP T-IIU which is a medium sized tokamak with a 0.91m major radius and 0.23m minor radius.

2. Zeeman polarimeter

Figure 1 shows a schematic diagram of the newly developed Zeeman polarimeter. This measuring system consists of a photoelastic modulator(PEM), band-pass filter(BF), polarizing beam splitter(PBS), Fabry-Perot interferometer(F-P) and photomultiplier tubes(PMT1,2).

The Fabry-Perot interferometer scans a selected wavelength in the spectral line profile by changing the distance between a etalon with a piezoelectric element. The time resolution of the polarimeter was improved up to 1.5ms by using this interferometer in the measuring system. The left-hand and right-hand circular polarizations are converted to the linear polarizations orthogonal to each other(I_L and I_R) by the photoelastic modulator and the liner polarizations are separated with a polarizing beam splitter and detected separately with the photomultiplier tubes. The two photomultiplier tubes are located far from the plasma by using optical fibers purposing not to pick up various noises due to the hard X-ray and so on. These output signals are processed by a computer for data analysis, being converted to the line profile signal(I_L+I_R) and the modulation signal(I_L-I_R) proportional to the magnetic field strength. The signals are subtracted and analyzed through the procedure based on Fast Fourier Transfer(FFT) to obtain the modulation signal(I_L-I_R) with high S/N ratio. The line profile signal(I_L+I_R) is produced by adding output signals.

3.Experimental result

Figure 2(a) shows the time evolution of the plasma current, the line profile(I_L+I_R) and the modulation(I_L-I_R) during the current ramp up(CRU). One of the many peaks in the line profile is shown in Fig.2(b). Figure 2(c) indicates the corresponding modulation. In these figures, the solid line expresses the results for fitting with one Gaussian and two shifted Gaussians respectively. We can get three experimental data; the maximum intensity of the line profile:I_0, the full width at half-maximum(FWHM) of the line:$\Delta\lambda$ and max(I_L-I_R) from the two fitting lines and can easily estimate the poloidal magnetic field using the equation

$$B_p = C \times \frac{\max(I_L - I_R)}{I_0} \times \Delta\lambda \quad (1)$$

where C is a constant decided from a calibration of the polarimeter. Figure 3(a) shows the time evolution of the poloidal magnetic field measured at a location very close to the plasma boundary. The solid line expresses the poloidal magnetic field due to the measured total plasma current. Since both are in good agreement, it can be said that the measuring accuracy of the polarimeter is sufficiently high.

In order to obtain the local poloidal magnetic field, the Abel inversion is applied to the measured profiles of poloidal magnetic field. Figure 3(b) shows the time evolution of the poloidal magnetic field profiles at the times indicated by the three arrows in Fig.3(a). We can find clearly the production of a skin current profile.

4.Summary

We have developed the Zeeman polarimeter for measuring the internal poloidal magnetic field with a high time resolution up to 1.5ms. We could successfully obtain the detailed time evolution of the internal poloidal magnetic field profile even during a rapid current ramping in JIPP T-IIU. As a result, we confirmed the clear production of skin current.

Reference

[1] K.Toi *et al*, Nucl.Fusion. **12**, 1643(1979).

[2] K.Toi *et al*, Phys.Rev.Lett. **64**, 1895(1990).

[3] M.C.Zarnstorff *et al.*, *Plasma Physics and Controlled Nuclear Fusion Reseach,1990* (International Atomic Energy Agency, Vienna, 1991), Vol. 1, p.109.

[4] L.L.Lao,J.R.Ferron *et al.*, Phys.Rev.Lett. **70**, 3435(1993).

[5] G.T.Hoang, C.Gil *et al.*, Nucl.Fusion. **34**, 75(1994).

[6] T.Fukuda and the JT-60 Team, Phys Plasmas. **2**, 2249(1995).

[7] H.Kuramoto, N.Hiraki *et al* ., J.Plasma Fusion Res.**71**, 1020(1995).

[8] U.Feldman, J.F.Seely, N.R.Sheeley, Jr., S.Suckewer and A.M.Title, J.Appl.Phys.**56**, 2512(1984).

[9] D.Wroblewski, L.K.Huang, and H.W.Moos, Rev.Sci.Instrum.**59**, 2341(1988).

[10] K.Toi et al.,in Plasma Physics and Controlled Nuclear Fusion Research (Proc. 13th Int. Conf. Washington D.C.,1990)Vol.1, p. 301,IAEA,Vienna (1991).

Figure caption

Fig.1 Schematic diagram of the Zeeman polarimeter on JIPP T-IIU tokamak. PEM : PhotoElastic Modulator, BF : Band-pass Filter, PBS : Polarizing Beam Splitter, F-P : Fabry-Perot interferomter, PMT1,2: PhotoMultiplier Tubes.

Fig.2 Output signal after data analysis and data fitting. (a) Time evolution of a plasma current, Line Profile(I_L+I_R) and Modulation(I_L-I_R) of the spectral line. (b) The line profile signal and (c) the circular polarization modulation signal. The solid lines are fitted profiles with Gaussians.

Fig.3 Time evolution of poloidal magnetic field and the inverted poloidal magnetic field profiles in JIPP T-IIU. (a) Circle is the measured poloidal magnetic field. The solid line is the poloidal magnetic field from total plasma current. (b)Circles shows the profile before CRU; squares, during CRU; lozenge, after CRU.

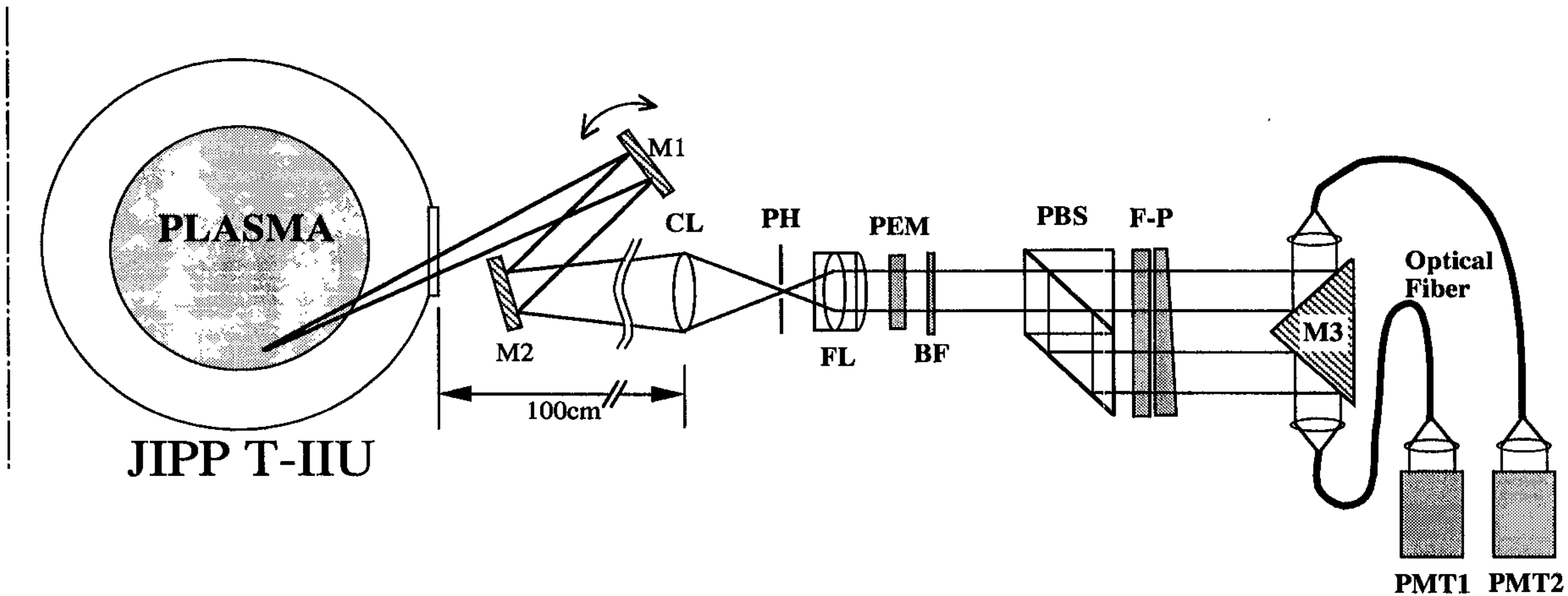
PLASMA
JIPP T-IIU
M1
M2
100cm
CL
PH
FL
PEM
BF
PBS
F-P
M3
Optical
Fiber
PMT1
PMT2

Fig.1

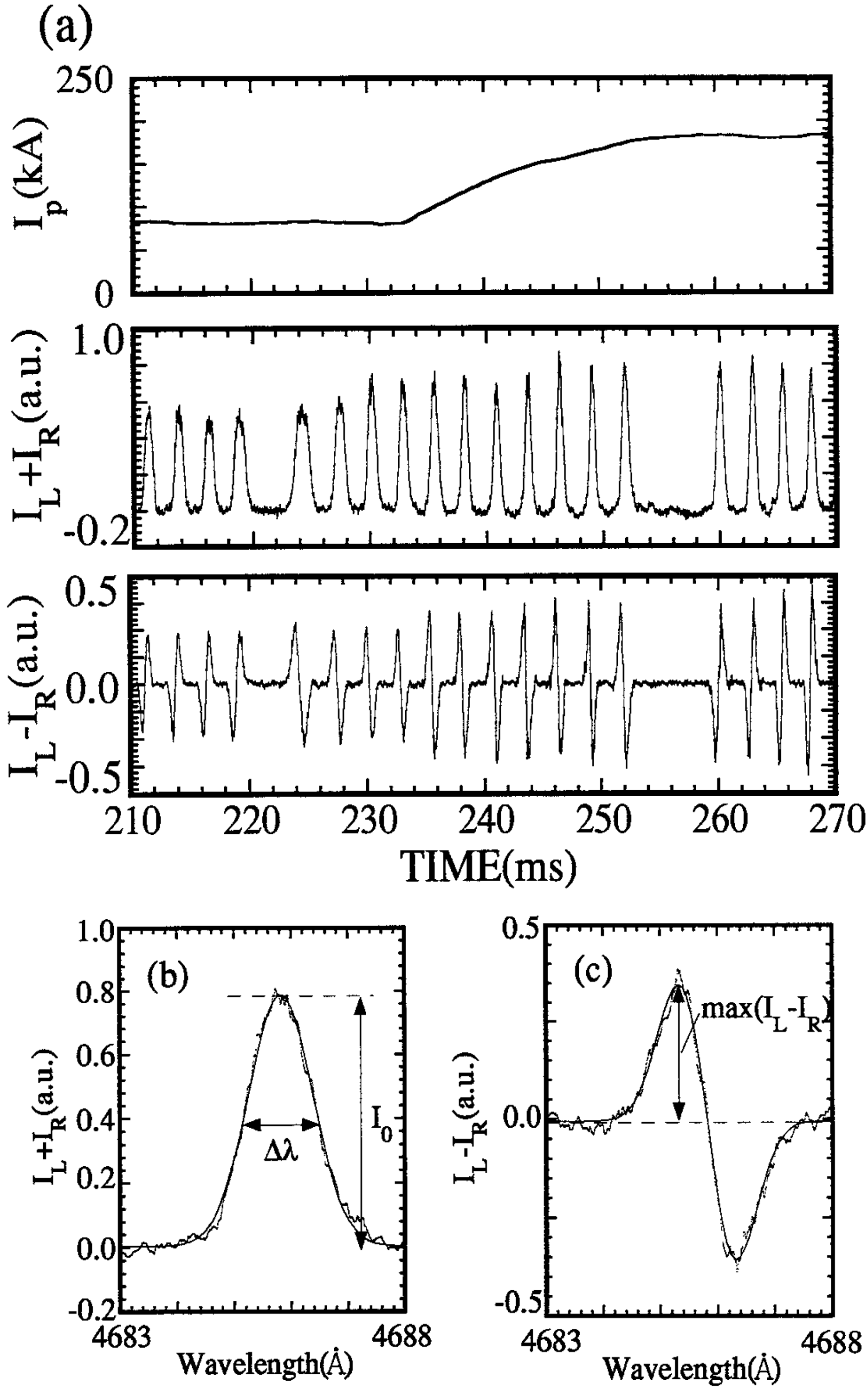

(a)
250
0
I_p(kA)
1.0
-0.2
I_L+I_R(a.u.)
0.5
0.0
-0.5
I_L-I_R(a.u.)
210
220
230
240
250
260
270
TIME(ms)
(b)
1.0
0.8
0.6
0.4
0.2
0.0
-0.2
I_L+I_R(a.u.)
Δλ
I_0
4683
4688
Wavelength(Å)
(c)
0.5
0.0
-0.5
I_L-I_R(a.u.)
max(I_L-I_R)
4683
4688
Wavelength(Å)

Fig.2

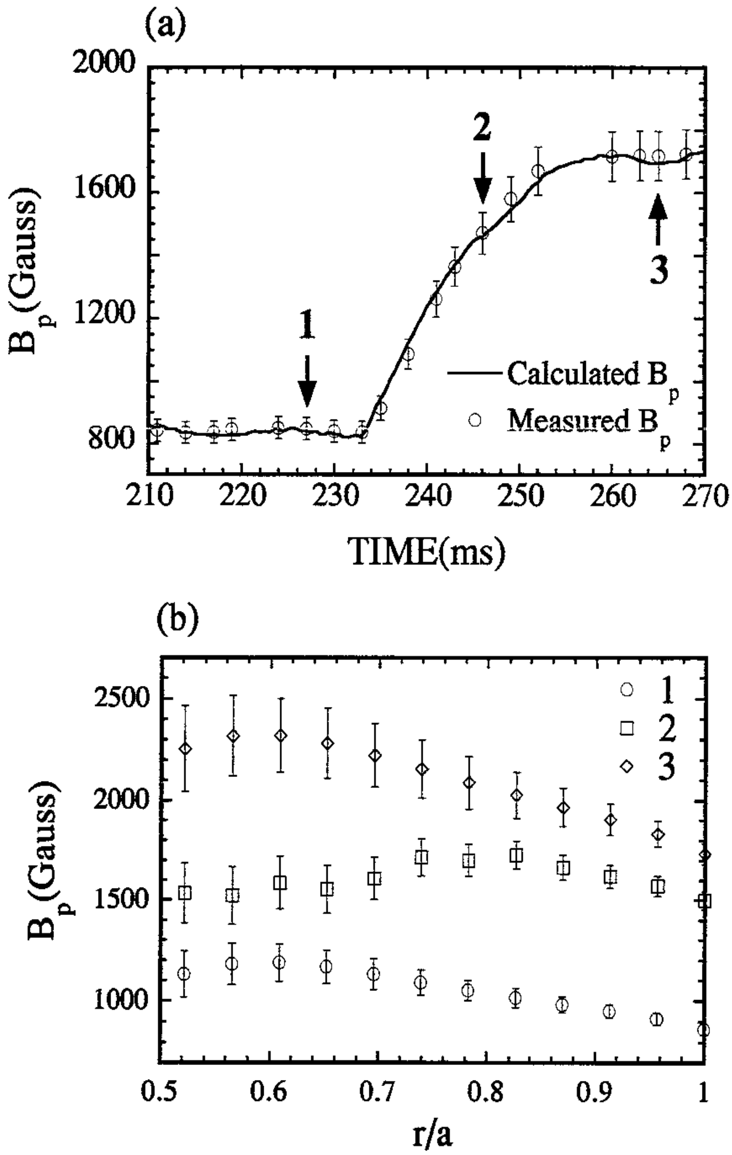

(a)
2000
1600
1200
800
B_p (Gauss)
1
2
3
Calculated B_p
Measured B_p
210
220
230
240
250
260
270
TIME(ms)
(b)
2500
2000
1500
1000
B_p (Gauss)
1
2
3
0.5
0.6
0.7
0.8
0.9
1
r/a

Fig.3

Recent Issues of NIFS Series

NIFS-351 J. Uramoto,
An Estimation of Life Time for A Low Energy Negative Pionlike Particle Beam: Apr. 1995

NIFS-352 A. Taniike,
Energy Loss Mechanism of a Gold Ion Beam on a Tandem Acceleration System: May 1995

NIFS-353 A. Nishizawa, Y. Hamada, Y. Kawasumi and H. Iguchi,
Increase of Lifetime of Thallium Zeolite Ion Source for Single-Ended Accelerator: May 1995

NIFS-354 S. Murakami, N. Nakajima, S. Okamura and M. Okamoto,
Orbital Aspects of Reachable β Value in NBI Heated Heliotron/Torsatrons; May 1995

NIFS-355 H. Sugama and W. Horton,
Neoclassical and Anomalous Transport in Axisymmetric Toroidal Plasmas with Electrostatic Turbulence; May 1995

NIFS-356 N. Ohyabu
A New Boundary Control Scheme for Simultaneous Achievement of H-mode and Radiative Cooling (SHC Boundary); May 1995

NIFS-357 Y. Hamada, K.N. Sato, H. Sakakita, A. Nishizawa, Y. Kawasumi, R. Liang, K. Kawahata, A. Ejiri, K. Toi, K. Narihara, K. Sato, T. Seki, H. Iguchi, A. Fujisawa, K. Adachi, S. Hidekuma, S. Hirokura, K. Ida, M. Kojima, J. Koong, R. Kumazawa, H. Kuramoto, T. Minami,. M. Sasao, T. Tsuzuki, J.Xu, I. Yamada, and T. Watari,
Large Potential Change Induced by Pellet Injection in JIPP T-IIU Tokamak Plasmas; May 1995

NIFS-358 M. Ida and T. Yabe,
Implicit CIP (Cubic-Interpolated Propagation) Method in One Dimension; May 1995

NIFS-359 A. Kageyama, T. Sato and The Complexity Simulation Group,
Computer Has Solved A Historical Puzzle: Generation of Earth's Dipole Field; June 1995

NIFS-360 K. Itoh, S.-I. Itoh, M. Yagi and A. Fukuyama,
Dynamic Structure in Self-Sustained Turbulence; June 1995

NIFS-361 K. Kamada, H. Kinoshita and H. Takahashi,
Anomalous Heat Evolution of Deuteron Implanted Al on Electron Bombardment; June 1995

NIFS-362 V.D. Pustovitov,
Suppression of Pfirsch-schlüter Current by Vertical Magnetic Field in Stellarators; June 1995

NIFS-363 A. Ida, H. Sanuki and J. Todoroki
An Extended K-dV Equation for Nonlinear Magnetosonic Wave in a Multi-Ion Plasma; June 1995

NIFS-364 H. Sugama and W. Horton
Entropy Production and Onsager Symmetry in Neoclassical Transport Processes of Toroidal Plasmas; July 1995

NIFS-365 K. Itoh, S.-I. Itoh, A. Fukuyama and M. Yagi,
On the Minimum Circulating Power of Steady State Tokamaks; July 1995

NIFS-366 K. Itoh and Sanae-I. Itoh,
The Role of Electric Field in Confinement; July 1995

NIFS-367 F. Xiao and T. Yabe,
A Rational Function Based Scheme for Solving Advection Equation; July 1995

NIFS-368 Y. Takeiri, O. Kaneko, Y. Oka, K. Tsumori, E. Asano, R. Akiyama, T. Kawamoto and T. Kuroda,
Multi-Beamlet Focusing of Intense Negative Ion Beams by Aperture Displacement Technique; Aug. 1995

NIFS-369 A. Ando, Y. Takeiri, O. Kaneko, Y. Oka, K. Tsumori, E. Asano, T. Kawamoto, R. Akiyama and T. Kuroda,
Experiments of an Intense H- Ion Beam Acceleration; Aug. 1995

NIFS-370 M. Sasao, A. Taniike, I. Nomura, M. Wada, H. Yamaoka and M. Sato,
Development of Diagnostic Beams for Alpha Particle Measurement on ITER; Aug. 1995

NIFS-371 S. Yamaguchi, J. Yamamoto and O. Motojima;
A New Cable -in conduit Conductor Magnet with Insulated Strands; Sep. 1995

NIFS-372 H. Miura,
Enstrophy Generation in a Shock-Dominated Turbulence; Sep. 1995

NIFS-373 M. Natsir, A. Sagara, K. Tsuzuki, B. Tsuchiya, Y. Hasegawa, O. Motojima,
Control of Discharge Conditions to Reduce Hydrogen Content in Low Z Films Produced with DC Glow; Sep. 1995

NIFS-374 K. Tsuzuki, M. Natsir, N. Inoue, A. Sagara, N. Noda, O. Motojima, T. Mochizuki, I. Fujita, T. Hino and T. Yamashina, *Behavior of Hydrogen Atoms in Boron Films during H_2 and He Glow Discharge and Thermal Desorption;* Sep. 1995

NIFS-375 U. Stroth, M. Murakami, R.A. Dory, H. Yamada, S. Okamura, F. Sano and T. Obiki,
Energy Confinement Scaling from the International Stellarator Database; Sep. 1995

NIFS-376 S. Bazdenkov, T. Sato, K. Watanabe and The Complexity Simulation Group,
Multi-Scale Semi-Ideal Magnetohydrodynamics of a Tokamak Plasma; Sep. 1995

NIFS-377 J. Uramoto,
Extraction of Negative Pionlike Particles from a H2 or D2 Gas Discharge Plasma in Magnetic Field; Sep. 1995

NIFS-378 K. Akaishi,
Theoretical Consideration for the Outgassing Characteristics of an Unbaked Vacuum System; Oct. 1995

NIFS-379 H. Shimazu, S. Machida and M. Tanaka,
Macro-Particle Simulation of Collisionless Parallel Shocks; Oct. 1995

NIFS-380 N. Kondo and Y. Kondoh,
Eigenfunction Spectrum Analysis for Self-organization in Dissipative Solitons; Oct. 1995

NIFS-381 Y. Kondoh, M. Yoshizawa, A. Nakano and T. Yabe,
Self-organization of Two-dimensional Incompressible Viscous Flow in a Friction-free Box; Oct. 1995

NIFS-382 Y.N. Nejoh and H. Sanuki,
The Effects of the Beam and Ion Temperatures on Ion-Acoustic Waves in an Electron Beam-Plasma System; Oct. 1995

NIFS-383 K. Ichiguchi, O. Motojima, K. Yamazaki, N. Nakajima and M. Okamoto
Flexibility of LHD Configuration with Multi-Layer Helical Coils; Nov. 1995

NIFS-384 D. Biskamp, E. Schwarz and J.F. Drake,
Two-dimensional Electron Magnetohydrodynamic Turbulence; Nov. 1995

NIFS-385 H. Kitabata, T. Hayashi, T. Sato and Complexity Simulation Group,
Impulsive Nature in Collisional Driven Reconnection; Nov. 1995

NIFS-386 Y. Katoh, T. Muroga, A. Kohyama, R.E. Stoller, C. Namba and O. Motojima,
Rate Theory Modeling of Defect Evolution under Cascade Damage Conditions:The Influence of Vacancy-type Cascade Remnants and

Application to the Defect Production Chracterization by Microstructural Analysis; Nov. 1995

NIFS-387 K. Araki, S. Yanase and J. Mizushima,
Symmetry Breaking by Differential Rotation and Saddle-node Bifurcation of the Thermal Convection in a Spherical Shell; Dec. 1995

NIFS-388 V.D. Pustovitov,
Control of Pfirsch-Schlüter Current by External Poloidal Magnetic Field in Conventional Stellarators: Dec. 1995

NIFS-389 K. Akaishi,
On the Outgassing Rate Versus Time Characteristics in the Pump-down of an Unbaked Vacuum System; Dec. 1995

NIFS-390 K.N. Sato, S. Murakami, N. Nakajima, K. Itoh,
Possibility of Simulation Experiments for Fast Particle Physics in Large Helical Device (LHD); Dec. 1995

NIFS-391 W.X.Wang, M. Okamoto, N. Nakajima, S. Murakami and N. Ohyabu,
A Monte Carlo Simulation Model for the Steady-State Plasma in the Scrape-off Layer; Dec. 1995

NIFS-392 Shao-ping Zhu, R. Horiuchi, T. Sato and The Complexity Simulation Group,
Self-organization Process of a Magnetohydrodynamic Plasma in the Presence of Thermal Conduction; Dec. 1995

NIFS-393 M. Ozaki, T. Sato, R. Horiuchi and the Complexity Simulation Group
Electromagnetic Instability and Anomalous Resistivity in a Magnetic Neutral Sheet; Dec. 1995

NIFS-394 K. Itoh, S.-I Itoh, M. Yagi and A. Fukuyama,
Subcritical Excitation of Plasma Turbulence; Jan. 1996

NIFS-395 H. Sugama and M. Okamoto, W. Horton and M. Wakatani,
Transport Processes and Entropy Production in Toroidal Plasmas with Gyrokinetic Eletromagnetic Turbulence; Jan. 1996

NIFS-396 T. Kato, T. Fujiwara and Y. Hanaoka,
X-ray Spectral Analysis of Yohkoh BCS Data on Sep. 6 1992 Flares - Blue Shift Component and Ion Abundances -; Feb. 1996

NIFS-397 H. Kuramoto, N. Hiraki, S. Moriyama, K. Toi, K. Sato, K. Narihara, A. Ejiri, T. Seki and JIPP T-IIU Group,
Measurement of the Poloidal Magnetic Field Profile with High Time Resolution Zeeman Polarimeter in the JIPP T-IIU Tokamak; Feb. 1996